Science Advances
AAAS

Supplementary Materials for

Autonomous, untethered gait-like synchronization of lobed loops made from liquid crystal elastomer fibers via spontaneous snap-through

Dae Seok Kim *et al.*

Corresponding author: Shu Yang, shuyang@seas.upenn.edu; Dae Seok Kim, daeseok@pknu.ac.kr

Sci. Adv. **9**, eadh5107 (2023)
DOI: 10.1126/sciadv.adh5107

The PDF file includes:

Other Supplementary Material for this manuscript includes the following:

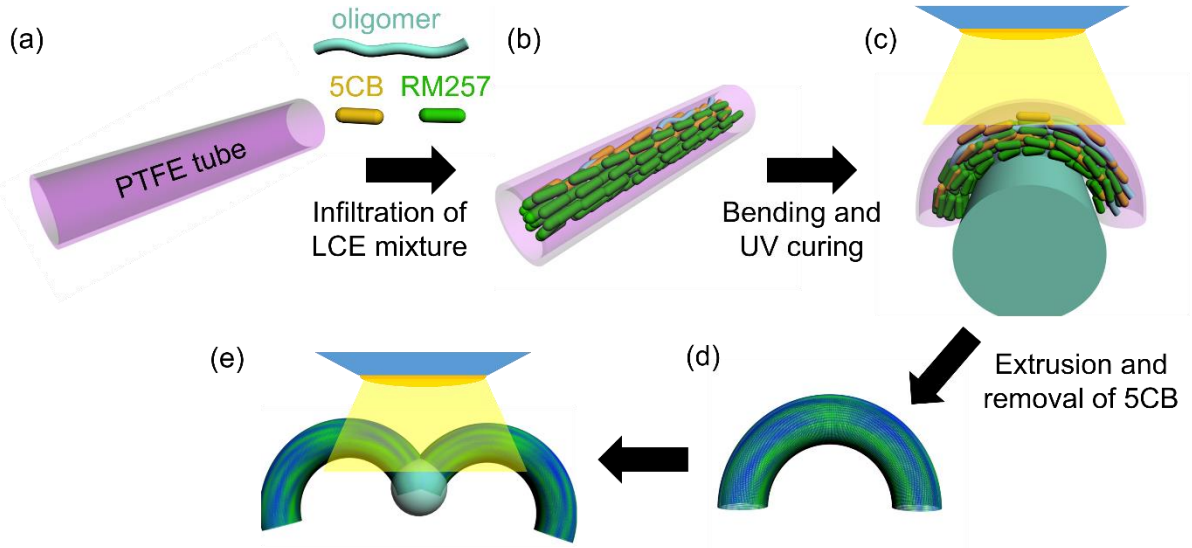

Fig. S1. Fabrication of a single pre-bent LCE fiber and their connection using glue. (a,b) Infiltration of LCE mixture into PTFE tube. (c) UV cross-linking process of the LCE fiber in a bent PTFE tube. (d,e) a Pre-bent LCE fiber and connected LCE fibers with glue bead.

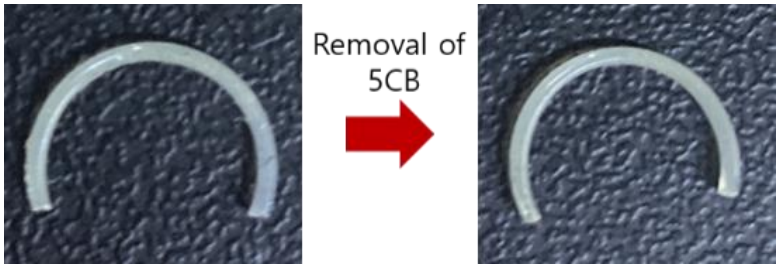

Fig. S2. Comparison of LCE fibers w/ and w/o removal of 5CB. Images of pre-bent LCE fiber (a) before and (b) after removal of 5CB.

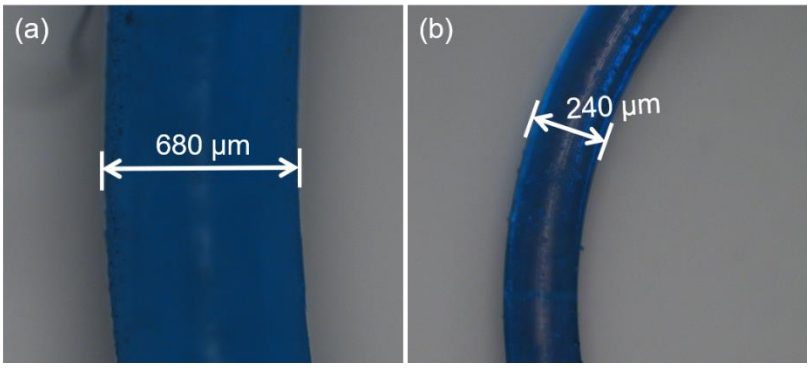

Fig. S3. Optical microscope images of the LCE fibers. LCE fibers with diameters of (a) ~680 and (b) ~240 μm, respectively.

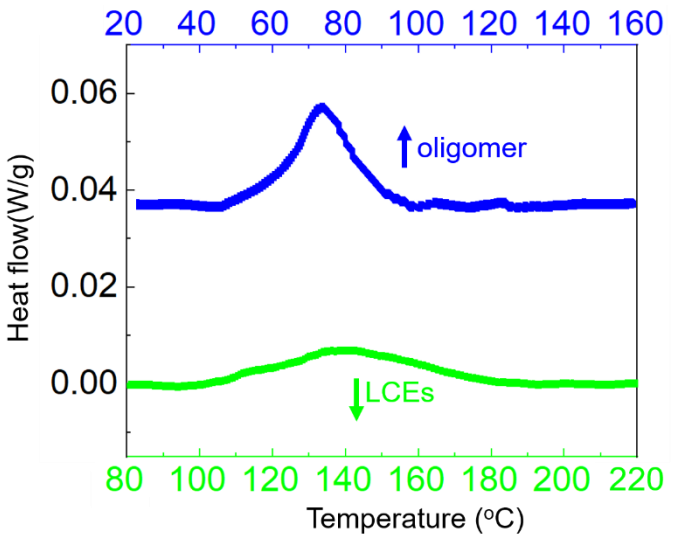

Fig. S4. DSC curves of RM82-1,3PDT oligomer and LCE without 5CB. The curves shows the transition temperature from nematic to isotropic phase at ~143℃.

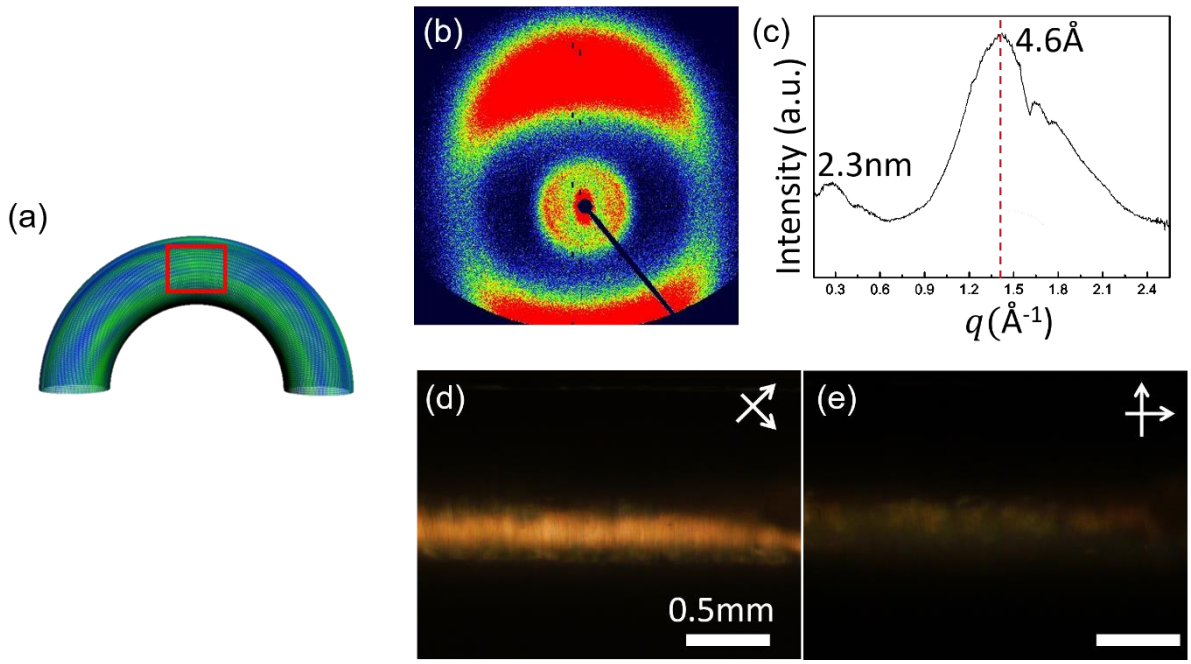

Fig. S5. Alignment characterization of the pre-bent LCE fiber. (a) Illustration of the pre-bent LCE fiber. (b) X-ray scattering patterns of the pre-bent fiber where the beam passed through the area denoted by red box in (a). (c) 1D profile of the azimuthally integrated 2D patterns of the pre-bent LCE fiber. (d,e) POM images of the pre-bent LCE fiber, focused on the area denoted by red box in (a).

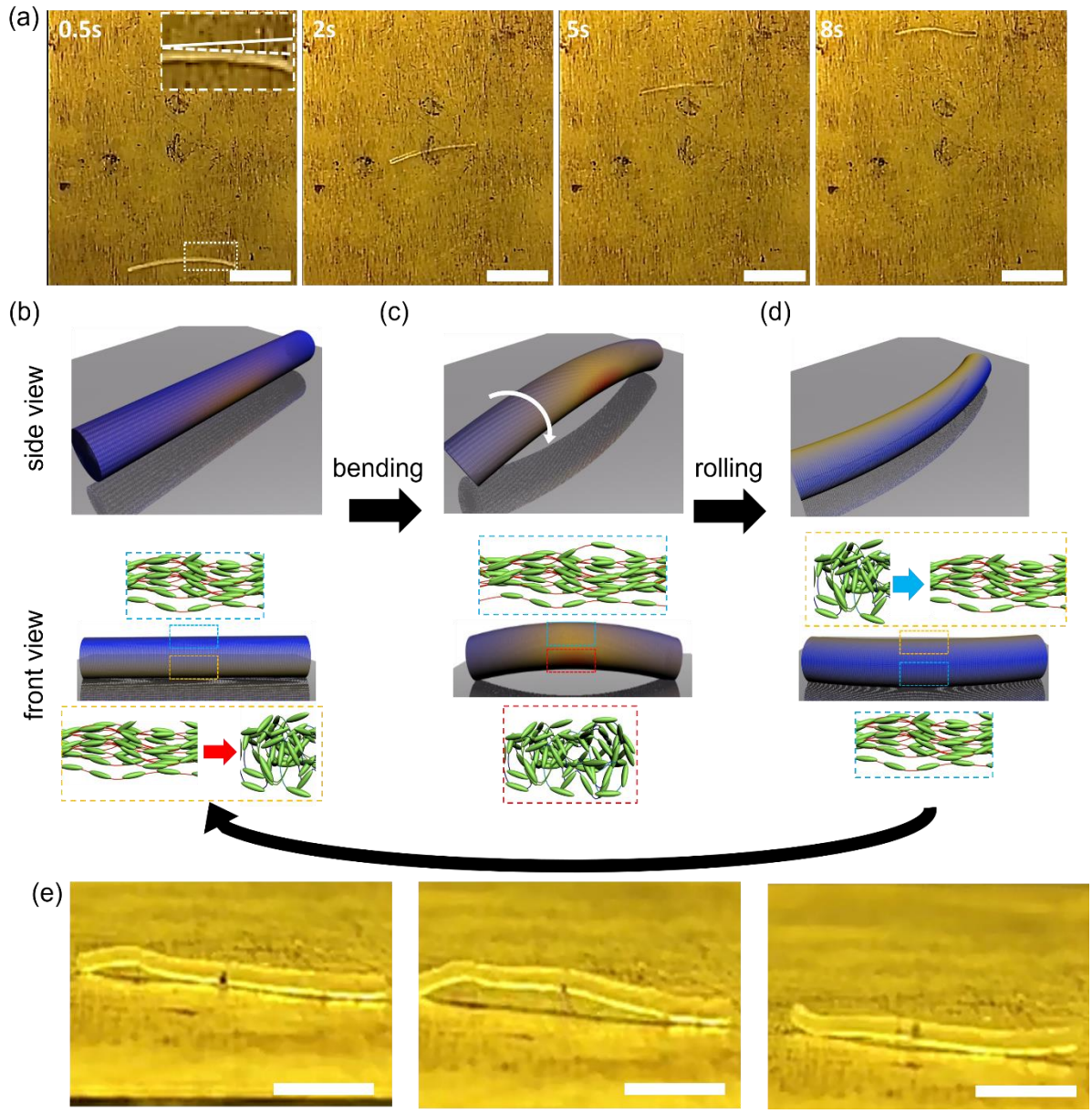

Fig. S6. Snapshots and corresponding illustrations of a slightly bent LCE fiber rolling. (a,e) Snap shots of the LCE fiber rolling on a hot plate at 200^{o}C from top and side view, respectively. All scale bars are 1 cm. (b-d) The corresponding illustration of the LCE fiber rolling.

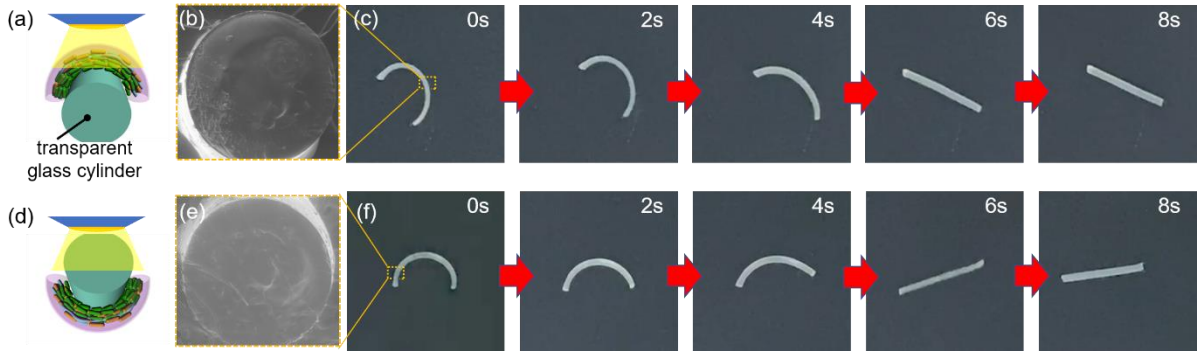

Fig. S7. Comparison of pre-bent fibers prepared by UV polymerization in opposite directions. (a,d) Sketches of UV-curing process, where they were cured in opposite direction of UV shinning. (b,d) Cross-sectional SEM images of the corresponding pre-bent fibers. (c,f) Thermally activated rotation of the corresponding pre-bent fibers onto a hot plate (170℃).

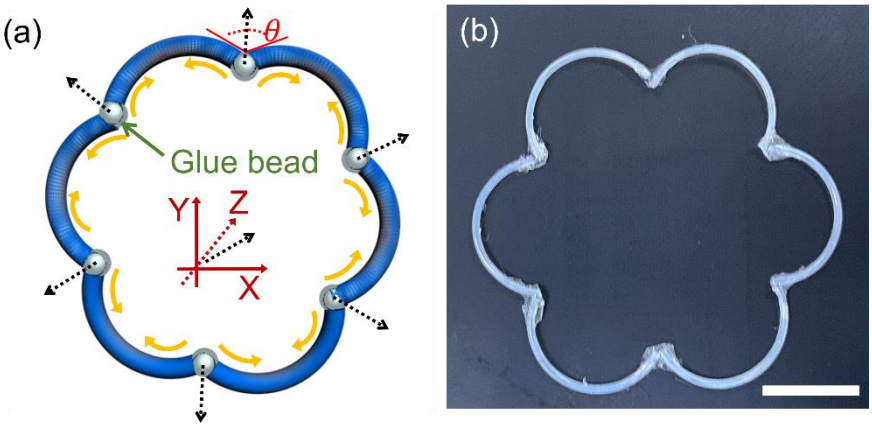

Fig. S8. Sketch and image of 6-lobed LCE loop. (a,b) Schematic illustration and the corresponding photographs of the 6-lobed LCE loop where the fibers are connected using UV-curable polymer glue. Here, θ is angle between adjacent two fibers and yellow arrows indicate direction of shrinkage during heating and the black dash arrows indicate the resulting direction of the connected part. The scale bar is 1 cm.

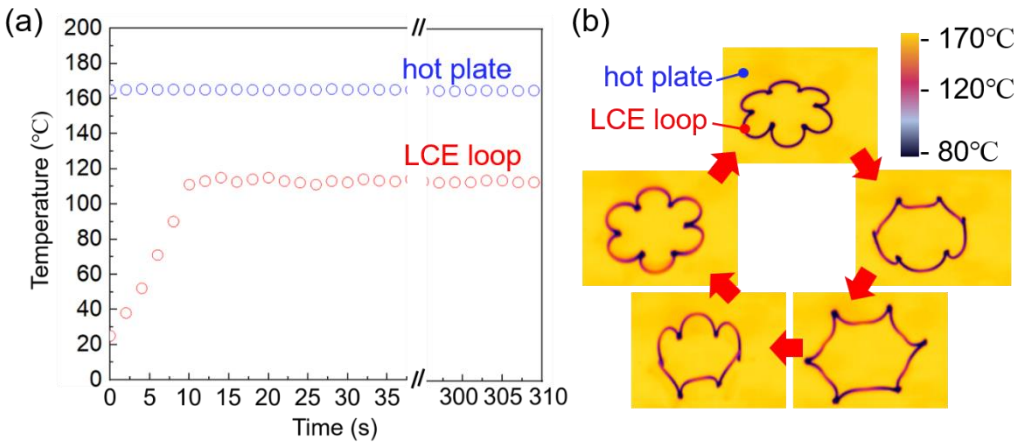

Fig. S9. Thermal analysis of 6-lobed LCE loop during flipping. (a) temperature profiles of 6-lobed LCE loop flipping and hot plate as a function of time. (b) The corresponding IR images of the LCE loop flipping, which were taken at ~8-10s.

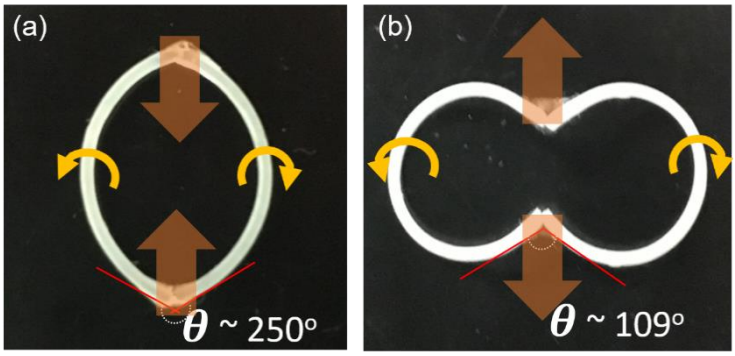

Fig. S10. 2-lobed LCE loops with different θ. Images of the 2-lobed LCE loop with (a) $\theta \sim 250^{O}$ and (b) $\theta \sim 109^{O}$.

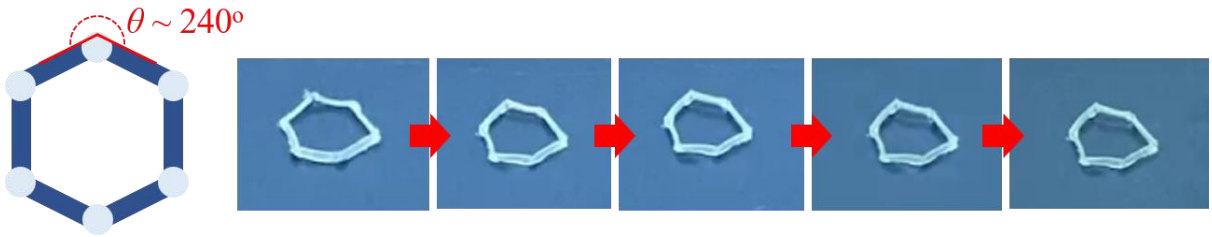

Fig. S11. Schematic illustration and snap shots of a hexagon LCE loop attempting to move on the hot plate (170℃).

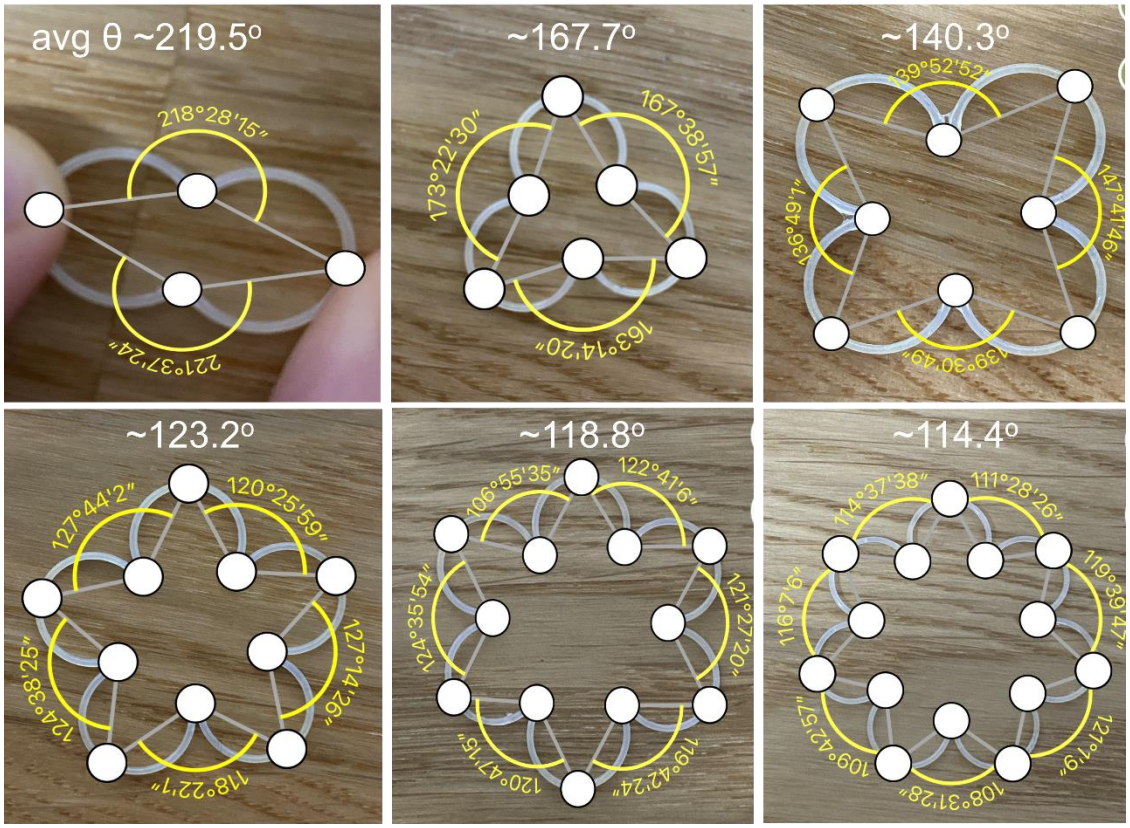

Fig. S12. Images of 2- to 7-fold lobed LCE loops with average angles between connected fibers.

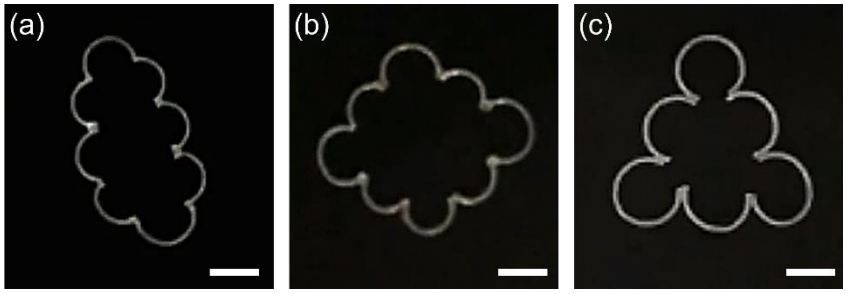

Fig. S13. Snap-shots of anisotropic shapes of lobed LCE loops. (a) elliptical, (b) rhombus and (c) triangular arrangement. All scale bars are 1 cm.

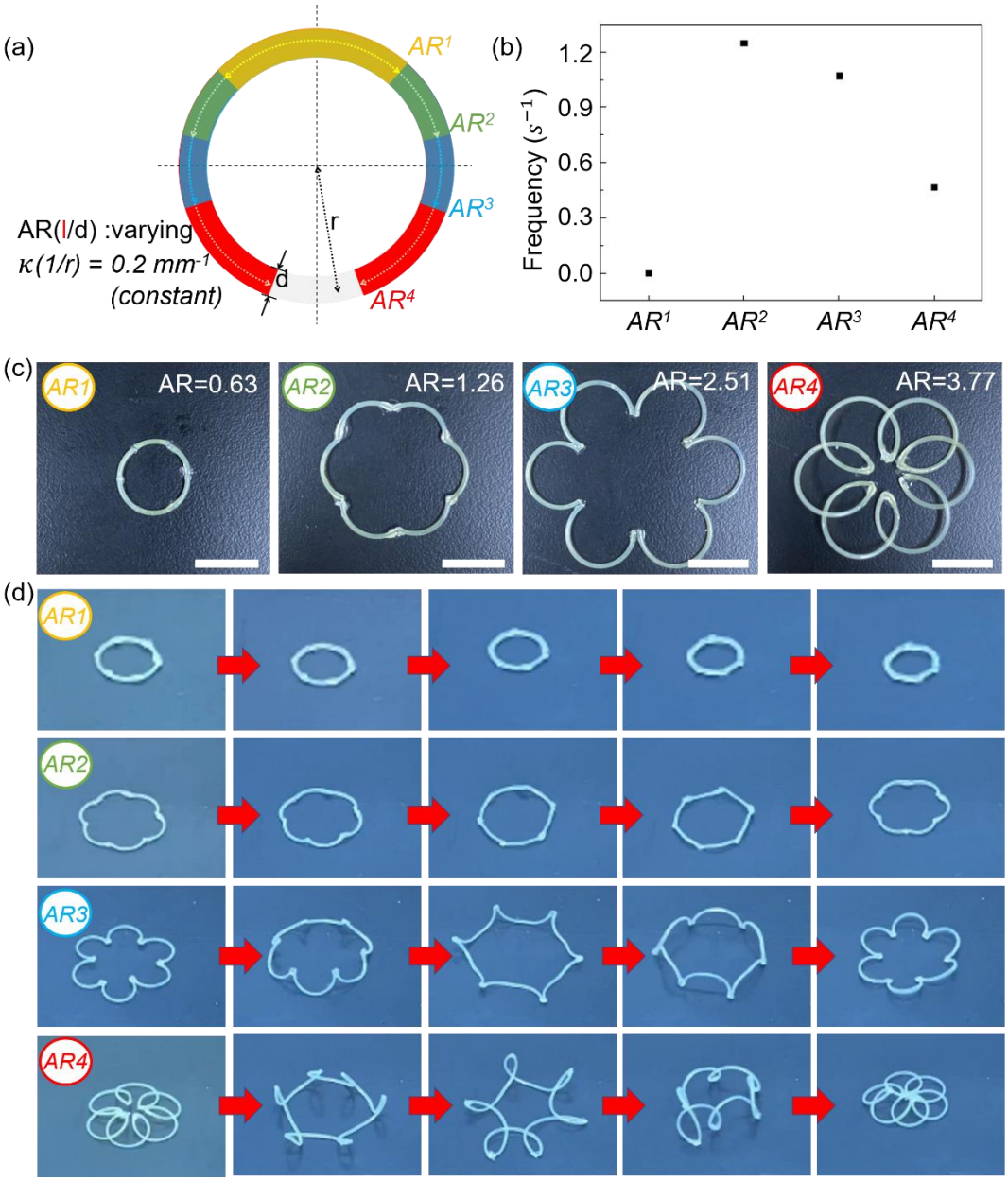

Fig. S14. Flipping behaviors of the 6-fold lobed LCE loops with varying aspect ratios (length/diameter) and a constant curvature. (a) Sketch of pre-bent fibers AR1 to AR4, where aspect ratio varies with only length. (b) The flipping frequency of the 6-lobed loops made from pre-bent fibers AR1 to AR4. (c) Images of the corresponding the 6-lobed loops. All scale bars are 1μm. (d) Snapshots of the single flipping cycle of the 6-lobed loops.

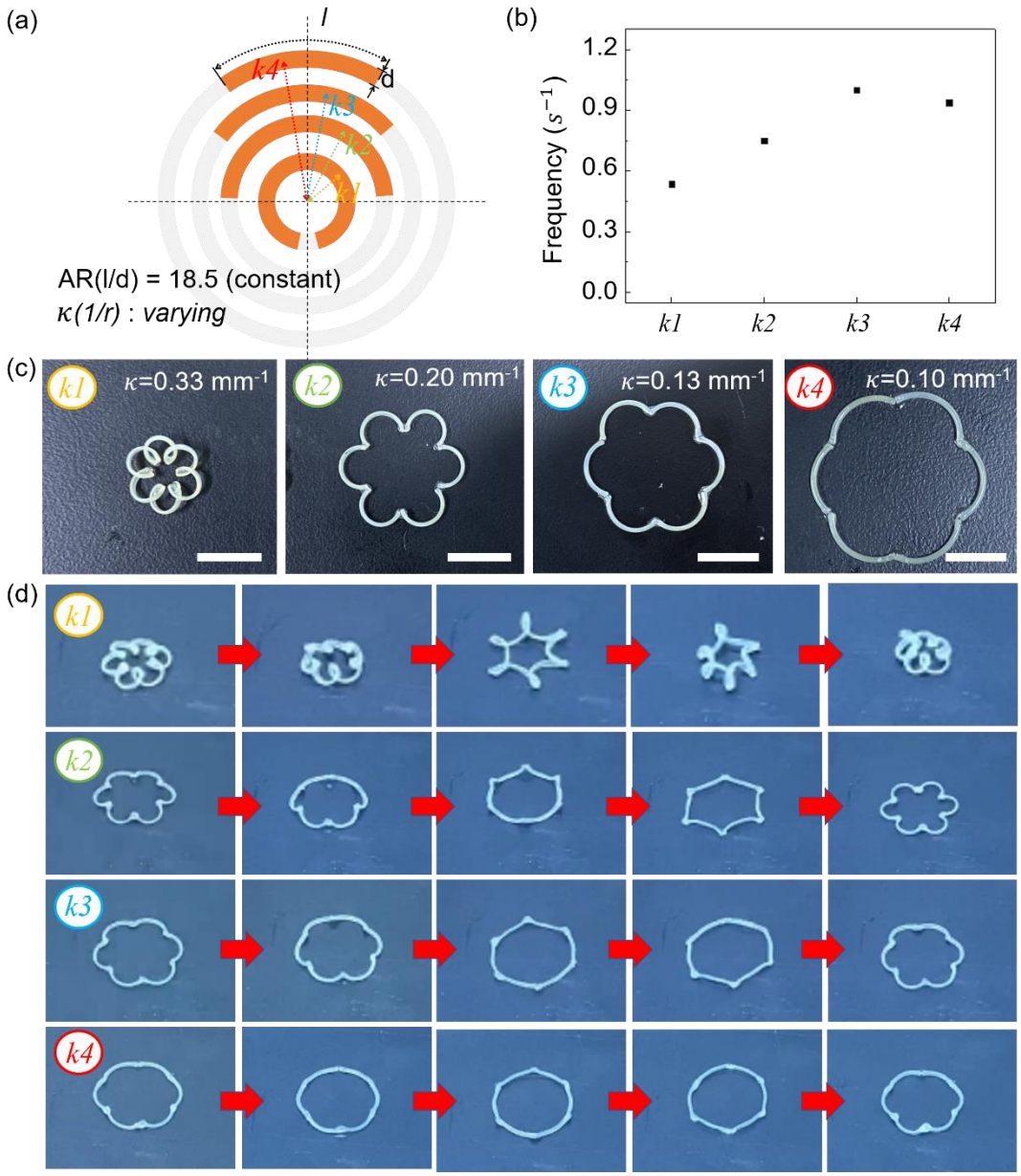

Fig. S15. Flipping behaviors of the 6-fold lobed LCE loops with varying curvatures and a constant aspect ratio. (a) Sketch of pre-bent fibers *k*1 to *k*4, where radii of pre-bent fibers vary with constant aspect ratio 18.5. (b) The flipping frequency of the 6-lobed loops made from the pre-bent fibers *k*1 to *k*4. (c) Images of the corresponding the 6-lobed loops. All scale bars are 1μm. (d) Snapshots of single flipping cycle of the 6-lobed loops.

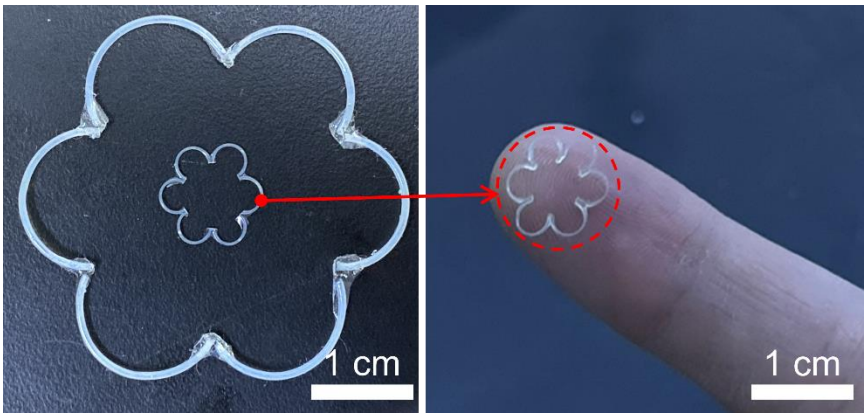

Fig. S16. Snap-shots of a 6-fold lobed loop made of pre-bent fibers with different size. Each fiber of small and large LCE loops presents diameter of 250 μm and length of 4 mm, respectively.

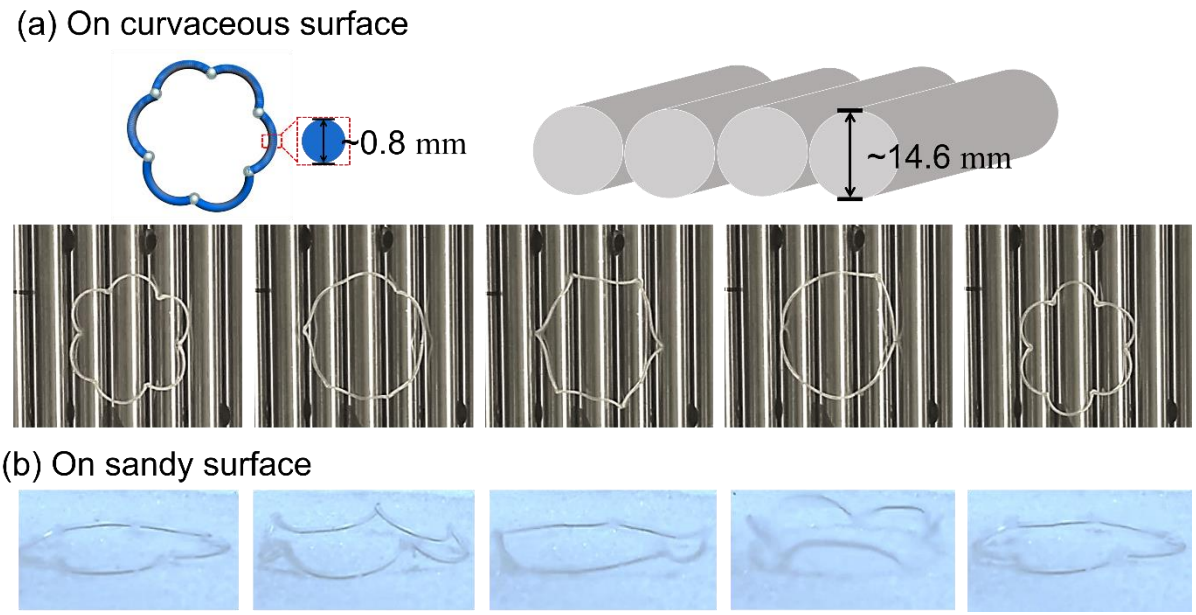

Fig. S17. The Synchronized locomotion of 6-fold lobed loop on different terrains. (a) On curvaceous surface. (b) On sandy surface.

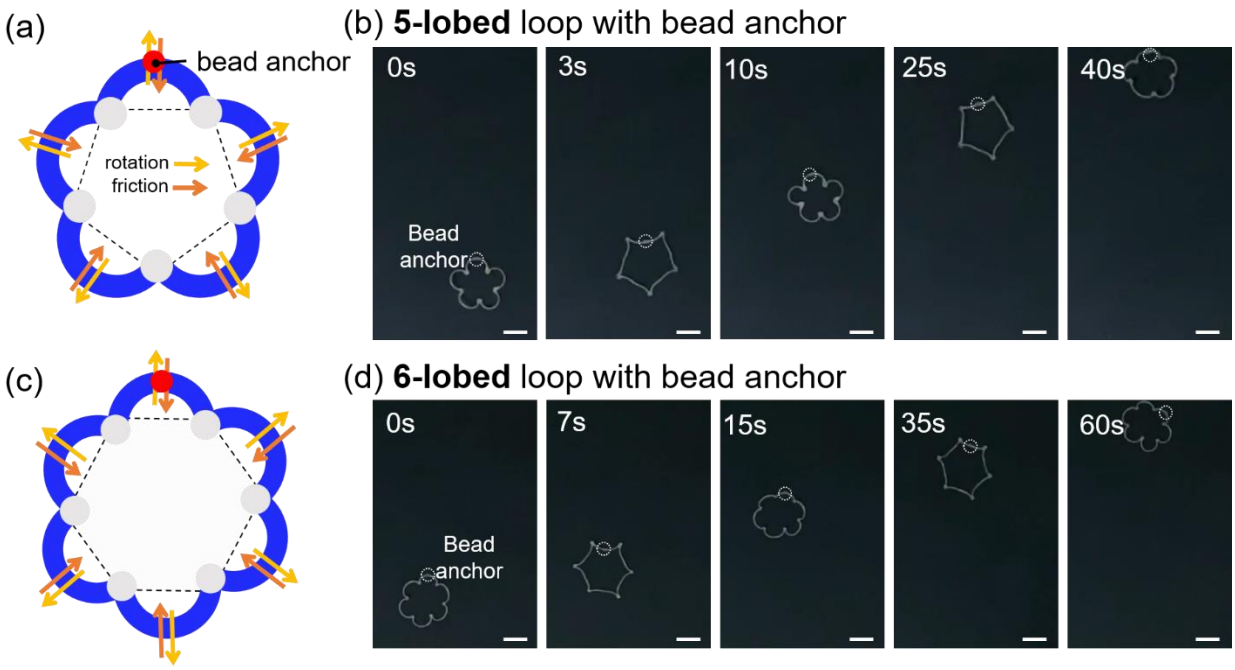

Fig. S18. Comparison of directional movements between 5- and 6-lobed LCE loops. (a,c) sketches and (b,d) snapshots of 5- and 6-lobed LCE loops moving forward, respectively, which of movement is directed with the bead anchor. All scale bars are 1cm.

Video S1. The rolling of pre-bent LCE fiber on a hot plate at 200 ℃

Video S2. The comparison of cylindrical and rectangular shape of LCE fiber.

Video S3. The waddling gait of 2-lobed fiber on hot plate at 170 ℃

Video S4. The synchronized flipping of the 6-fiber loop on hot plate at 170 ℃.

Video S5. The self-sustainable flipping of the 6-fiber loop on hot plate at 170 ℃ for an hour long

Video S6. The synchronized flipping of the 6-fiber loop on hot plate at 110 ℃ below the $T_{N\text{-}I.}$

Video S7. FEM simulation of the synchronized flipping of the 6-fiber loop.

Video S8. Thermal shrinkage of the LCE loop surrounded with a copper wire by joule heating

Video S9. 2-lobed LCE loops with varying θ, above and below 180°.

Video S10. The synchronized flipping of 2- to 7-fold lobed LCE loops.

Video S11. The synchronized flipping of lobed loops in elliptical, rhombus and triangular arrangement.

Video S12. The synchronized flipping of small 6-lobed loop made of pre-bent fibers of 250 μm in diameter and 4 mm in length.

Video S13. Synchronized locomotion of 6-fold lobed loop on hot curvaceous and sandy surfaces.

Video S14. The directional movement of 5-fold lobed loop on hot plate at 150 and 180 ℃.

Video S15. The climbing of 5-fold lobed loop on a slope of 18^{o}.

Video S16. Soft robots using the LCE loops as soft propulsion leg.